Materials Advances

ROYAL SOCIETY OF CHEMISTRY

PAPER

View Article Online
View Journal | View Issue

Cite this: *Mater. Adv.*, 2024, 5, 3706

Developing tuneable viscoelastic silicone gel-based inks for precise 3D printing of clinical phantoms†

Gloria Nieva-Esteve, [a] Núria Agulló,[a] Miguel Grande-Molina,[bc] Núria Adell,[d] Xavier Tarrado,[e] Laura Calvo-Duarte,[b] Arnau Valls-Esteve, [d] Lucas Krauel,[e] Felip Fenollosa-Artés, [bc] Robert Texidó Bartes *[a] and Salvador Borrós [a]

Tissue and organ phantoms with realistic anatomical features are becoming increasingly popular in the medical field due to their potential to revolutionize surgical planning and practice. Despite advancements in the production technology using 3D printing and development of materials, the availability of 3D printable materials that accurately replicate human organs' mechanical properties is limited. Therefore, we developed a family of silicone gel-based inks that can be 3D printed using direct ink writing (DIW) with tuneable viscoelastic properties that mimic a wide range of soft tissues. The control over viscoelastic properties is achieved by fine tuning of silicone formulations with a rheology modifier to promote the encapsulating silicone oil. This strategy not only allows for the recreation of the viscoelastic behaviour profile of a wide range of soft tissues through amplitude and frequency sweeps but also is entirely compatible with DIW printing for medical model manufacturing. Thus, this study stands as one of the few in the literature presenting a DIW printing technology enabling the printing of silicone with such precise control over viscoelastic properties that it allows for different sensations to be experienced by the evaluating medical team.

Received 5th January 2024,
Accepted 28th February 2024

DOI: 10.1039/d4ma00011k

rsc.li/materials-advances

1. Introduction

Tissue and organ phantoms with realistic anatomical features are becoming increasingly popular in the medical field, particularly for preoperative planning, medical training, and patient understanding.[1] These models accurately simulate biological structures, providing surgeons with a safe environment to practice and fine-tune their skills, as well as providing a versatile platform for training and testing.[2] In addition, tissue and organ phantoms are cost-effective,[3] easier to manipulate than traditional tools such as virtual reality, and more ethical and precise than animal models.[4] Particularly, 3D-printed tissue and organ phantoms are rapidly gaining popularity in the medical field,[5] with a growing number of research studies and clinical trials highlighting their potential to revolutionize surgical planning[6–10] and practice.[11–15]

Despite widespread interest, serious constraints prevent phantoms that mimic human tissues and exhibit realistic behaviour from becoming a reality. Firstly, from a manufacturing perspective, phantoms have been created using traditional techniques such as casting.[16–18] These technologies are time-consuming and costly due to the need for tooling preparation and waste disposal.[19] As a result, personalized medical phantoms for individual patients are often impractical due to the high cost and time of production. Instead, most of these models are produced in large quantities as generalized, idealized versions for educational purposes that are not personalized. Additionally, these moulded phantoms lack the ability to precisely replicate internal characteristics and complex features of the human anatomy, such as blood vessels or nerve structures, making it difficult to accurately visualize the anatomical reality.[20]

3D printing technologies offer a solution to the limitations of traditional manufacturing processes, as they allow for the rapid and cost-effective production of patient-specific, high-fidelity medical phantoms without the need for tooling.[21]

[a] *Grup d'Enginyeria de Materials (GEMAT), Institut Químic de Sarrià, Universitat Ramon Llull, Via Augusta, 390, Barcelona 08017, Spain. E-mail: robert.texido@iqs.url.edu*
[b] *Centre CIM, Universitat Politècnica de Catalunya (CIM UPC), Carrer de Llorens i Artigas, 12, 08028, Barcelona, Spain*
[c] *Universitat Politècnica de Catalunya, Carrer de Jordi Girona, 31, Barcelona 08034, Spain*
[d] *Hospital Sant Joan de Déu, Esplugues de Llobregat, Spain*
[e] *Urology Unit, Pediatric Surgery Department, Hospital Sant Joan de Déu, Universitat de Barcelona, Spain*

† Electronic supplementary information (ESI) available. See DOI: https://doi.org/10.1039/d4ma00011k

These technologies offer a solution to the challenge of replicating the intricacy of anatomical structures by producing high-resolution phantoms, making it the primary manufacturing technique for medical phantom fabrication. Despite 3D printing technologies' potential, they are currently hindered by limitations in the availability of 3D printable materials that can accurately replicate the mechanical properties of human organs and tissues. From a materials perspective, conventional 3D phantoms are composed of commercially available materials such as thermoplastics,[22–24] and polymer resins,[25,26] due to their straightforward production process; however, their mechanical properties are vastly different from those of soft tissues found in the human body.[5] This mismatch in the mechanical properties can limit the realism of conventional 3D phantoms and compromise their usefulness for certain medical applications. It has been demonstrated that practising on materials that are harder than the tissue can lead to an increase in surgical complications due to the use of excessive force during surgery.[27] Consequently, although they reproduce anatomical structure complexity, they still fall short in replicating the full biomechanical complexity. For this reason, these models are useful for visualizing and learning anatomy, but they cannot be used for surgical planning[28] and rehearsal because they do not represent the true texture of tissues.

In this sense, 3D printing technologies, such as the J850 Digital Anatomy printer from Stratasys S.L, try to recreate the softness and density of native tissues by unique material combination[29,30] or playing with the infill density and pattern.[31–33] However, they are focused on replicating specific properties such as Young's modulus values, shore hardness,[34] tensile strength, density or elasticity.[5] This approach oversimplifies the models using simple mechanical models to be compared with soft tissues. Therefore, it fails to capture the complexity of biomechanical soft tissues which are highly complex materials that exhibit viscoelastic behaviour,[35] which means that their mechanical properties change in response to different loading rated and time-dependent deformations, especially when tissue touch and cutting sense has to be recreated. In addition, this viscoelasticity is frequency-dependent, meaning that the mechanical properties of the tissue change with the frequency of the applied force. To create phantoms that can serve as tactile tools for presurgical planning, it is necessary to avoid using simple mechanical models that assume linear and elastic behaviour, and accurately characterize the viscoelasticity of soft tissues[36] in terms of both elasticity and viscosity[34] depending on the frequency applied. Therefore, not only the processability through 3D printing techniques is required to precisely recreate the anatomic regions, but also a deeper understanding of the viscoelastic properties of soft tissues will improve the phantom realistic surgeon feelings. Despite meeting materials performance requirements and overcoming technological limitations, the clinical utility of these models is yet to be fully established due to a lack of validation from healthcare professionals. All the issues raised above suggest that despite significant advancements in fabrication technologies and available materials, there are still limitations in creating organ phantoms with desired mechanical and physicochemical properties to mimic soft tissues. Therefore, a compromise between the ability to recreate anatomical morphology and the recreation of physical characteristics is still necessary.

In this context, lots of studies have used hydrogels to fabricate phantoms using 3D printing. Hydrogels are three-dimensional networks of hydrophilic polymers that display viscoelasticity and can absorb and retain a large amount of water. These trapped water molecules act as a lubricant and allow the polymer chains to move and slide more easily, giving them viscoelastic properties. In addition to their similarity in mechanical properties, hydrogels can also be tailored easily, mimicking the geometrical, architectural, and mechanical features of soft tissues. For example, Desheng Liu *et al.*[37] developed a 3D printable tissue-mimicking elastomeric double network hydrogel that matches Young's modulus of diverse biological soft tissues by regulating the composition of the hydrogel matrix and the density of metal coordinator bonds.[37] Additionally, Wang *et al.*[38] used a combination of GelMA/HAMA inks and DLP-based 3D printing to create a range of complex soft tissues with a compressive modulus similar to those of actual tissues with high structural sophistication and accuracy. Moreover, Hinton *et al.*[39] developed a method for 3D printing biological structures such as arterial branches using alginate, collagen, and fibrils gels as inks and gelatin slurry as the support. The technique achieved a resolution of about 200 μm, but the stiffness was found to be higher than the human brain or lungs. Leibinger *et al.*[40] compared two different models that try to mimic brain tissue: while gelatin models show insertion forces that agree closely to the brain, composite hydrogel models better mimic the viscous nature of this soft tissue. Both materials match different characteristics of the brain, but neither of them is a perfect substitute. The aforementioned studies serve as examples describing the utility of hydrogels as a material for fabricating medical phantoms; however, they also show that hydrogels have also certain limitations and drawbacks that must be considered such as the limited shelf-life, and variability in their properties depending on small variations of the manufacturing process.[41] Additionally, biopolymers are not stable for long term use and allow bacterial growth in a material.[42]

Silicone can be used as an alternative to hydrogels for 3D printing medical phantoms due to its viscoelasticity, durability, thermal stability, and higher tensile strength especially when compared with hydrogels. These properties are important because, phantoms are often used in procedures or tests that involve exposure to heat or changes in temperature, therefore, thermal stability is required. In addition, they are often subjected to repeated use and handling, and they need to withstand the stresses of manipulation and testing without degrading over time, hence, long durability in combination with mechanical stability is necessary. And finally, high tensile strength ensures that they can maintain their shape and properties during use, which is essential for accurate and reliable testing and training that involve stretching, pulling

and compressing the sample. Thus, these properties are important for creating long-lasting and realistic phantoms that accurately simulate the properties of human tissues. For example, silicone has been used to replicate the internal structure of the human bronchial vasculature[43] due to its versatility in tensile strength (ranging from 0.2 to 165 MPa, with PDMS being the gold standard at 5 MPa),[44] and elongation at break (5% to 1490%).[44] However, intrinsic issues of silicone processing, such as its high viscosity for formulations of higher elastic modulus, and the complexity of controlling the polymerization reaction, make it more challenging to process silicone formulations through 3D printing, relegating the fabrication of complex structures to more simple fabrication procedures such as casting.

In this study, we developed a family of UV photocurable silicone gel-based inks that meet the stringent requirements for producing realistic medical phantoms. These inks have advantageous qualities that successfully address the primary issues encountered in phantom manufacturing. They are specifically compatible with direct ink writing (DIW) technology, feature tuneable viscoelastic properties that effectively imitate the tactile sensations of various soft tissues, and have been tested by a multidisciplinary team of surgeons. The achievement of these properties is attributed to tight control over the silicone gel structure, which achieves a compromise between rheological properties important for material processing and the viscoelastic behaviour of the material. Our approach employs a modification of the photocurable silicone network to accurately reproduce the elastic and viscous modulus profiles of several soft tissues, such as the brain, kidney, muscle, and cartilage, by encapsulating different amounts of silicone oil. Furthermore, considerable improvements in printability are achieved by the addition of fumed silica. Finally, we conducted assessments with a team of surgeons from Sant Joan de Déu Children's Hospital, who are known for their expertise in 3D simulation and surgical planning, to evaluate the capabilities of the printed medical phantoms to simulate tissue behaviour during medical procedures. Using a survey-based approach, surgeons evaluated the realism of our materials in replicating the tactile experience of soft tissues and executing surgical activities such as cutting and suturing. This examination not only sheds information on the relationship between the recreated viscoelastic properties and tissue behaviour, but it also emphasises the significant advantage that our materials give over available alternatives for soft tissue replication.

2. Materials & method

2.1. Materials

Commercial liquid silicone rubber (LSR 2060) obtained from Momentive has been used in this study. This silicone is a photocurable silicone that cures *via* a platinum-catalysed system under UV light. UV light initiates the hydrolysation reaction[45] between silicone polymer chains and the curing agent.[46] To produce a silicone gel, non-commercial polydimethylsiloxane (silicone oil) with a viscosity of 1000 Cst is added to the mixture. The methyl group[47] terminating silicone oil polymer chain is non-reactive. Thus, they do not participate in the silicone network formation during the curing reaction and remain encapsulated in the silicone network. Aerosil 200® (purchased from EVONIK), a hydrophilic fumed silica widely utilized in industry to control the rheology and thixotropy of liquids, binders, and polymers,[48] is included in the mixture as a reinforcing agent. Nivea Créme® is used as the gold standard of printable materials for extrusion printing. 3D-printed DragonSkin silicone 2ShoreA is used as a control for surgeons' clinical validation given that it is the gold standard phantom material.

2.2. General procedure for the synthesis of silicone formulations

Silicone inks are prepared using a liquid silicone in combination with a 5% of commercial catalyst. Different quantities of non-commercial silicone oil are added to generate different viscoelastic properties (from 0 to 10 ratio of silicone oil *versus* silicone). To improve printability and to ensure the long-term stability of 3D-printed silicone components, hydrophilic fumed silica is added to the formulations (at 0.05 g g^{-1}). The complete formulation details of each material can be found in Table S1 of the ESI.† A centrifugal mixer (Speedmixer DAC 600.2 FlakTek) blends all materials at 3000 rpm. for 3 min. To identify the different formulations used in this study, we have assigned them specific names based on their composition. Formulations composed of silicone and silicone oil are named SS, while those containing silicone, silicone oil, and hydrophilic fumed silica (Aerosil) are named SSA. The number that follows SS or SSA is the grams of silicone oil per gram of silicone.

2.3. Rheological properties to predict printability

The storage and loss modulus, the shear-thinning behaviour, and the recovery capacity of all the formulations were evaluated before curing to determine 3D printability. Rheological characterization of the silicone ink formulations was performed using an AR 2000 rheometer from TA Instruments. The rheometer was equipped with a flat 20 mm plate made of steel and the gap was fixed at 300 μm. The silicone ink samples were loaded onto the rheometer plate, ensuring that the entire gap was filled with silicone. To determine the linear viscoelastic region, an amplitude sweep was performed at 1 Hz from 0.1 to 100% strain. After this, a frequency sweep from 0.1 to 100 Hz at 2% strain was conducted to obtain consistency and information about the structure of the material. Shear thinning behaviour was determined by the evaluation of the viscosity across a shear rate ramp (from 0.02 to 2000 1 s^{-1}). The recovery test had three phases, the first one using a low shear rate (0.1 1 s^{-1}) to determine resting state viscosity, the second one at a high shear rate (100 1 s^{-1}) to determine viscosity when the material is flowing, and finally, the last step using the low shear rate, to show how quickly the material recovers the initial viscosity. All tests were performed at 25 °C.

2.4. 3D printing of silicone formulations

The silicone mixtures were loaded into 10cc opaque syringes barrels (Nordson EFD) minimizing air bubbles. Opaque nozzles

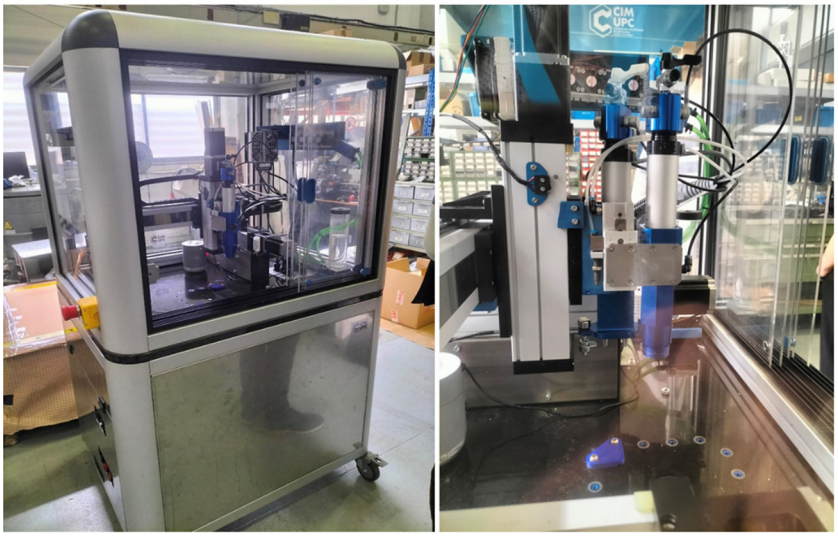

Fig. 1 PowerDIW 3D printer by CIM UPC. Details of the 3D printing moving part, DIW extrusion system and marble platform.

with a diameter of 0.58 mm were used for printing. Samples were printed using a direct ink writing (DIW) machine[49] (PowerDIW, CIM UPC, Barcelona, Spain) equipped with one DIW printheads inside a closed enclosure with temperature and humidity control (Fig. 1).

The same printing settings were used for all silicone-based formulations (SS0.5, SS1.8 and SSA7), including a layer height of 0.2 mm, a printing speed of 20 mm s^{-1}, two wall perimeters, and a 100% infill density. During the printing process, a UV photocuring process was employed using Hamamatsu UV light (LC-L1V5) at 7% (SSA0.5), 10% (SSA1.8) and 30% (SSA7) irradiance. This ensured optimal curing of each formulation keeping maximum shape fidelity. PDMS and other silicone samples have been processed to obtain solid specimens as described previously in other publications of the group.[50]

To assess printing resolution, a grid of 40 × 40 mm and a pore size of 4 × 4 mm are 3D printed. Filament diameters (verticals and horizontals) and pores sizes of each printed grid were quantified using Leica IC 3D. To assess printing resolution when fabricating a phantom model, a scaled kidney is printed using SSA0.5, SSA1.8 and SSA7. Mimics Materialise software was used to design a 3D kidney model, and PrusaSlicer was utilized for the slicing process.

To conduct a qualitative cutting and suturing tests by surgeons, two distinct samples were printed using a customized silicone 3D printer (called P3) created by CIM-UPC (further details can be found in the ESI† section). The samples consisted of semi-spheres (27 mm in diameter and 11 mm in height) and squares (55 × 55 mm squares and 3 mm in height). The printing parameters used are the same as 3D printed kidney phantoms except a concentric infill pattern was used to fabricate semi-spherical samples (Video S1, ESI†), while a rectilinear infill pattern was used for squares (Video S2, ESI†) to improve sample resolution. UV light at 7% (SSA0.5), 10% (SSA1.8) and 30% (SSA7) irradiance is used to ensure shape fidelity.

2.5. Viscoelastic behaviour determination

The viscoelastic behaviour of cured silicone formulations and tissues was carried out using dynamic mechanical analysis (DMA Q800 V21.2 TA) under frequency scans from 0.1 to 100 Hz at 2% strain using a compression clamp at 25 °C with a preload force of 0.5 N. Cylindrical samples with an approximate diameter of 13 mm were obtained from fresh organs and 3D-printed silicone samples. Fresh organs were purchased from local suppliers, and samples were obtained on the same day to ensure consistency and minimize any potential degradation of tissue properties. To capture the heterogeneity of the organs, efforts were made to select representative samples from various regions of each organ. The selected samples were carefully dissected to extract cylindrical tissue samples, ensuring uniformity in size and shape. Upon extraction, the samples were immediately placed in a refrigerated environment to maintain their freshness and structural integrity until tested. The thickness of all samples was approximately 3 mm to ensure consistency in the experimental setup. To account for variability within each organ, five replicates of each organ sample were obtained. This approach allowed for robust statistical analysis and enhanced the reliability of the experimental results. Similarly, 3D-printed silicone samples were fabricated to match the dimensions of the tissue samples, ensuring direct comparisons between biological and synthetic materials (13 mm of diameter and 3 mm of thickness).

2.6. Medical opinion. Protocol

Qualitative cutting and suture tests (Videos S3 and S4, ESI†) were performed by surgeons to assess the samples' suitability for surgical applications. To evaluate the usefulness, fidelity and experience of the surgeon using our formulations, a protocol of 8 questions has been developed that is valued from 1 to 5 (totally disagree to completely agree). On the other hand, each of the formulations has been evaluated as a candidate to

reproduce different tissues and organs (brain, adipose tissue, pancreas, kidney, liver, muscular tissue, skin, tumoral tissue and cartilage). Questions can be found in the ESI† section. In addition, each of the formulations has been compared with a commercial silicone (DragonSkin of 2ShoreA) that is already used to make phantoms to ensure the utility of our formulations. The protocol was followed by seven surgeons of Sant Joan de Déu Hospital.

3. Results and discussion

3.1. Optimization of silicone inks printability

Silicone-based ink formulations presented in this work compromise four main components that are crucial in controlling viscoelasticity while maintaining high printability using DIW techniques: silicone chains, platinum-catalysed curing agents, silicone oil and fumed silica (as shown in Fig. 2). The silicone chains and curing agent react under UV light to form a solid elastomeric network. Meanwhile, the silicone oil, which is composed of vinyl-terminated silicone chains, is encapsulated within the polymeric network to form a silicone gel with different viscoelastic properties compared to bulk silicone. Fumed silica, which are ceramic particles with a high specific surface area, are functionalized with hydroxyl groups on their surface. These groups promote the formation of hydrogen bonds with silicone oil chains, preventing their diffusion outside the polymeric network and promoting the thixotropic behaviour of the ink.

Despite the addition of silicone oil and Aerosil being explored before to modify bulk silicone, the optimization of the proportions of these components and the control over the tunability of the silicone is key to develop new inks with mimicking properties while processability using DIW. This led us to investigate the impact of silicone oil and Aerosil (fumed silica) on the rheological properties of the inks and their printability. In addition, this study aims to develop 3D printable inks that are versatile and can be used with different printers, including those with varying pressure forces. The challenge of developing such inks lies in the need to balance the viscosity and flow properties of the ink to ensure that it can be extruded consistently across different printers. To address these challenges, we will investigate the rheological properties of the ink.

To obtain good printability in DIW, the material must fulfil specific rheological behaviour where three main phases are identified: first, silicone ink must present a resting state, where it needs to have enough consistency to remain inside the syringe without leaking. Next, it undergoes a transition to a high shear state where it must flow while passing through the nozzle. Finally, it must quickly recover to its initial resting state properties to maintain the printed shape[51] (see Fig. 3A).

The key rheological properties that describe these three phases of the DIW process are the elastic and viscous moduli, viscosity related to shear thinning behaviour, and elastic recovery (Fig. 3B). By measuring the storage and loss moduli, we can assess the material's ability to withstand deformation during printing, which is critical for achieving accurate and high-quality 3D prints. They also indicate the elastic and viscous components of each formulation. Inks more elastic than viscous are desirable for 3D printing because it means that the material can be extruded and shaped without losing its shape or collapsing.

We also examined shear thinning behaviour, which is the behaviour of the fluid whose viscosity changes as it is subjected to increasing shear stress,[52] to ensure that the material can be extruded through the nozzle when shear stress is applied during the printing process. This property can be beneficial for 3D printing because it allows the material to flow more easily through the printer nozzle while still maintaining its shape once it exits the nozzle.

Finally, we conducted a recovery test where the materials are subjected to controlled deformation and then the extent to which the material recovers its original shape and properties after the deformation is measured. This information can provide insight into the material's ability to maintain its shape and mechanical properties during printing and can help to predict collapse during the printing process.

To assess whether our silicone-based formulations are suitable for 3D printing, we compared the rheological results with

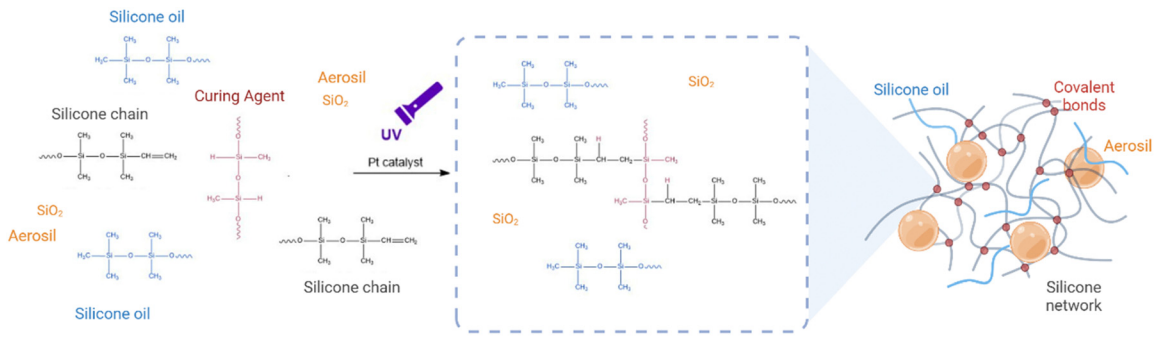

Fig. 2 Schematic overview of the strategy used in this paper. Precursors of photocurable LSR 2060 are silicone polymer chains (in grey) and platinum-catalysed curing agents (red). Silicone oil chains (in blue) and fumed silica (in orange) are incorporated into the mixture to obtain tuneable viscoelastic properties and 3D printability.

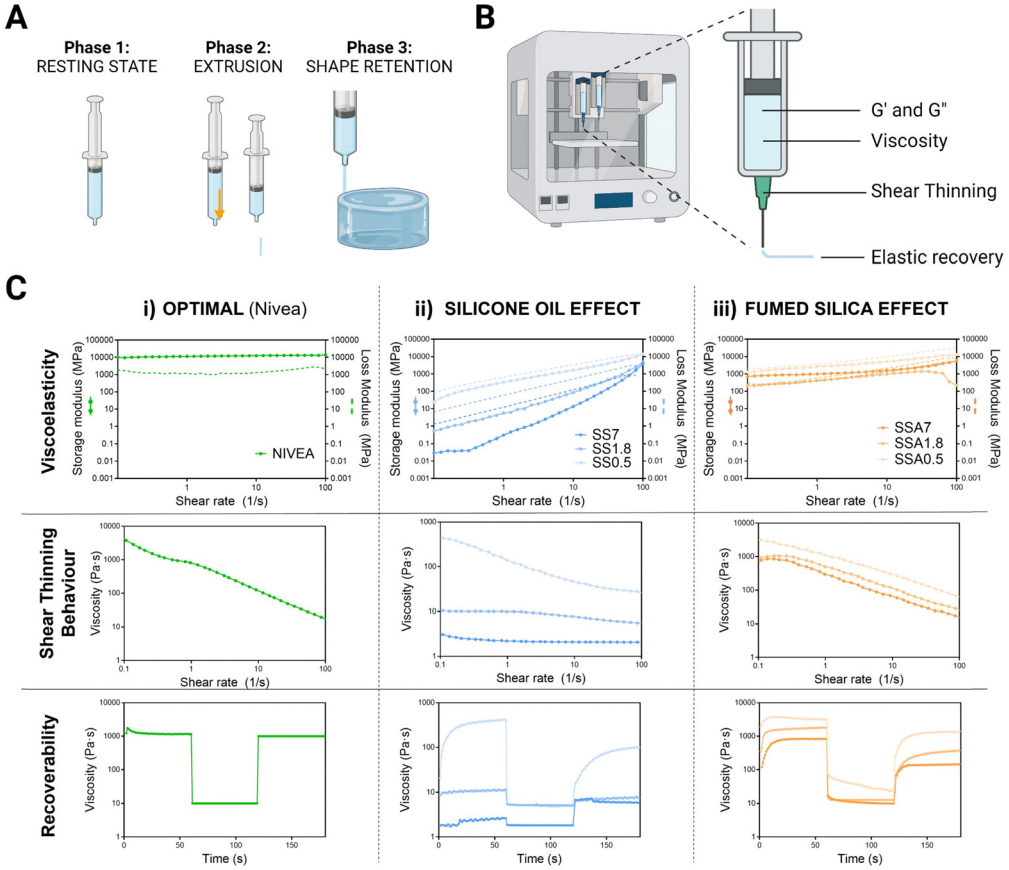

Fig. 3 Rheological properties affecting printability and shape fidelity in extrusion-based 3D printing. (A) Phases of materials extrusion in 3D printing. (B) Interplay of rheological properties. (C) Evaluation of the effect of silicone oil and fumed silica on elastic and viscous modulus, shear thinning behaviour and recoverability. (C)(i) Nivea Crème's results were used as a gold standard for rheological characterization. (C)(ii) Silicone oil effect on key rheological properties for extrusion-based 3D printing and the (C)(iii) effect of the incorporation of fumed silica to SS formulations. The data presented in each panel demonstrate the importance of these rheological properties in achieving high-quality, accurate prints.

those of Nivea Crème®, which has been used as a gold standard material for extrusion 3D printing in several studies[53,54] (Fig. 3C(i)). Nivea presents higher elastic than viscous moduli ensuring extrusion without losing integrity of the printed shape, shear thinning behaviour which guarantees fluidity and rapid recovery after deformation that assure shape fidelity.

The effect of silicone oil on the rheological properties of silicone inks has been studied an is shown in Fig. 3C(ii). First, the moduli were found to be frequency-dependent for all of them, increasing with increasing frequency as expected in viscoelastic materials. Later, it was found that silicone oil reduces elastic and viscous moduli, leading to less consistency and softness. Besides, the percentage of silicone oil is critical in determining the shear-thinning behaviour, as higher amounts do not display shear-thinning behaviour and instead present constant viscosity over the range of studied shear rates. The initial viscosity of these formulations was found to be insufficient in preventing leakage, with viscosities 50 or 100 times lower than optimal. The recovery test showed that increasing the ratio of silicone oil significantly reduced the initial viscosities, dropping the values to 10 Pa s, and no differences in viscosities are found between the three phases of the test, thus, they do not display recoverability. All these results are expected given that the viscosity of silicone oil is 600 times lower than silicone's viscosity. This leads to significant changes in the composition of the mixture as the percentage of silicone oil increases, making the silicone oil-based formulations unsuitable for 3D printing.

To address this, Aerosil 200® is added as an agent to regulate the rheological properties of silicone inks and optimized to display the optimum printable properties for DIW. As shown in Fig. 3C(iii), the addition of 0.05 g g^{-1} of Aerosil causes the convergence of moduli of all formulations, and the consistency of formulations with higher silicone oil percentages increases. This resulted in moduli very similar to Nivea Crème across the studied frequency range. The initial viscosities of all formulations increased and approached the initial viscosity of Nivea Crème. Moreover, viscosities decreased when the shear rate was increased, indicating shear thinning behaviour. In addition, all formulations showed flow behaviour and elastic recovery in the recovery test. Therefore, formulations containing fumed silica display favourable rheological properties for DIW printing regardless of silicone oil content. These promising results suggest that fine tuning of silicone

formulations is achieved, and they could be well-suited for the 3D printing of medical phantoms.

3.2. Printability through DIW

Printing resolution is crucial for 3D-printed medical phantoms to achieve accurate and reliable simulations of human anatomy and tissue properties, and for improving the accuracy and reliability of medical imaging and surgical procedures. As seen in rheology tests, silicone gel-formulations with high amounts of silicone oil are far from Nivea Crème rheological behaviour. Nevertheless, when fumed silica is incorporated into the formulations, they exhibit both shear-thinning behaviour, which is crucial for maintaining the ink's fluidity, and quicker recoverability, expecting better shape fidelity.

To corroborate these results, the resolution of the 3D printing process is evaluated using a 3D printed grid (Fig. 4A), which is the reference model to evaluate 3D printing resolution.[55–57] All formulations are used as inks to print this lattice and determine silicone oil and fumed silica effect over printability. The uniformity of filaments (Fig. 4Bi) is determined by quantifying the diameter of the filament along different points of the printed structure (d1, d2 and d3), and a smaller average value indicates a higher printing resolution. In addition, the standard deviation of the filament diameter of different regions provides insight into the uniformity of the deposited filament. Additionally, the transversal pore geometry is assessed (Fig. 4Bii) comparing the measured pore area from the printed sample with the pore area of the 3D model. Ideal filament stacking results in an optimal rectangular pore shape with a Printability Rate (Pr) value equal to 1. Printability rates below 1 indicates that the area of the final printed pores is higher than the ones designed in the 3D model revealing that the material of the filament flows narrowing the pore size.

The evaluation of printability of silicone inks can be qualitatively assessed through visualization of a printed reference grid. Fig. 4C shows that with low silicone oil concentrations (0.5 g silicone oil per g of silicone), a uniform filament is formed when extruding and a uniform lattice with differentiated filaments is formed when 3D printing. Increasing the silicone oil content had an undesired effect in terms of printability, given that a droplet is created when extruding and the pore size of the grid is reduced due to the inherent reduction of viscosity as observed in Fig. 3C(ii). Moreover, it was observed that formulations with high content of silicone oil do not present good printability because they exhibit collapsing during printing, and inconsistent and non-uniform patterns due to their low viscosity compromising the quality and accuracy of the printed object.

In good agreement with the rheological tests of Fig. 3C(iii), the incorporation of Aerosil prevents the silicone oil diffusion while viscosity is increased improving the filament uniformity when extruding for the whole range of studied formulations (Fig. 4C). During the printing process the filament flowed smoothly through the printer nozzle, maintaining the shape, adhering to the build platform and previous layers, and producing a finished part with dimensional accuracy, meeting the acceptable printability region. In addition, it is important to highlight that all the formulations with Aerosil, regardless of the amount of silicone oil, achieve very similar resolutions, although the printing parameters used to print them are the same. This indicates that fumed silica can be used to generate a wide range of printable silicone formulations with different

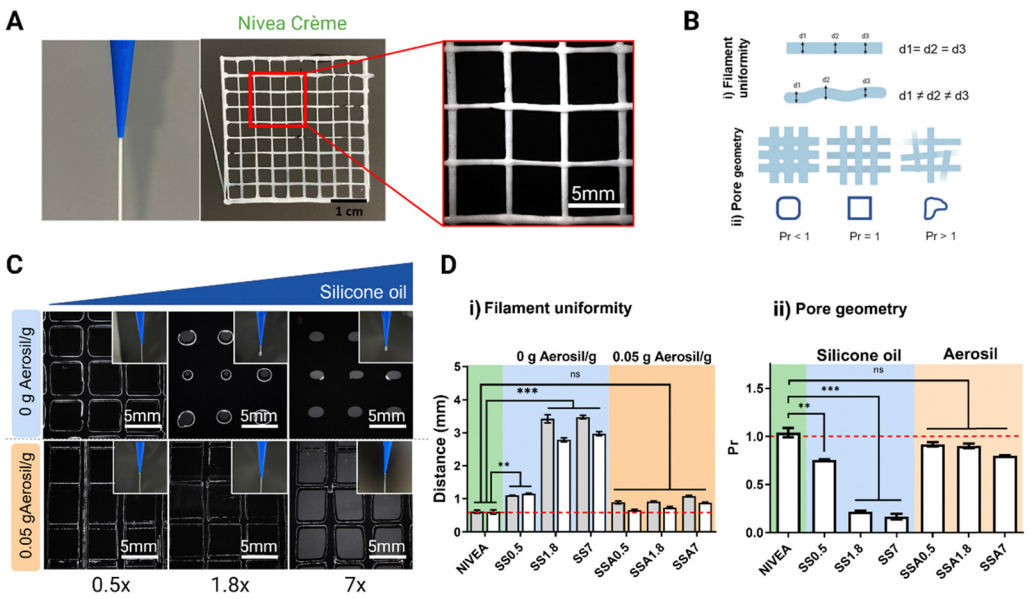

Fig. 4 Quantitative tests to assess the shape fidelity of inks during printing and post-fabrication. (A) 3D printed grid with silicone formulation to evaluate printability. (B) Quantitative tests for resolution. (B)(i) Filament uniformity of single filaments is evaluated by measuring the diameter's filament and homogeneity is characterized by comparing different measurements of the same fibre (d1, d2 and d3). (B)(ii) Planar structures evaluated on pore geometry with optimal rectangular pore shape (Printability index Pr = 1). (C) 3D printed grids using different silicone-based formulations to evaluate filament uniformity and pore geometry. (D)(i) Diameter of horizontal and vertical filament and (D)(ii) printability index of pore shape.

quantities of silicone oil while managing to facilitate the printing process. Fig. 4 presents the quantitative analysis of filament distance (Fig. 4D(i)) and Pr (Fig. 4D(ii)) of the 3D printed reference grid. Fig. 4D(i) shows that Nivea Crème filament distance is exactly the value of the nozzle diameter and the 3D model designed (0.58 mm) indicating this value as the maximum XY resolution achievable with the selected nozzle.

For formulations without Aerosil (0 g Aerosil g^{-1}), the filament distance increases proportional to the oil content, while, for formulations with Aerosil (0.05 g Aerosil g^{-1}) the filament distance values remain close to the 0.58 mm. Similarly, Fig. 4D(ii) show that Nivea Crème and Aerosil formulations exhibit a Pr = 1 or similar, while formulations without Aerosil exhibit a Pr value of lower than one, showing poor resolution. The results presented in this section match with the rheological study performed before, showing that rheology is an excellent and quick tool to predict 3D printability.

Although there are highly specific technologies that enable the printing of elastomeric materials using DIW with exceptionally high resolution (in the range of 50 μm),[58] the resolution of most DIW processes for processing silicone-based materials typically falls between 1000 and 100 μm.[59] Therefore, the resolution of our printing process is within standard parameters in DIW. Considering DIW processes where materials with storage and loss moduli are as low as those described in this article, resolutions around 1000–200 μm are found for the printing of hydrogel-based DIW. Hence, the resolution achieved in our prints also meets or exceeds standard resolution criteria.[60]

3.3. 3D printing of kidney phantoms as a proof of concept

Once it has been validated that all silicone gel formulations can be printed with good resolution, a proof of concept of a kidney phantom is fabricated using DIW 3D printing technology from a digital 3D model. To obtain this model, the first step was to import a computed tomography abdominal scan of a patient (DICOM file) into Materials Mimics software. There, the kidney was selected with manual segmentation, which is the process of extracting anatomical structures from medical images using an appropriate segmentation algorithm (in pink in Fig. 5A). Then, the software generated a 3D model of the organ by combining the segmented slices. The resulting 3D model is then utilized to evaluate the 3D printing resolution achievable with silicone-based formulation. As demonstrated in Fig. 5B the 3D printed phantom exhibits high fidelity to the 3D model in terms of its external and internal features such as internal cavities of the kidney. All silicone gel-based formulations containing Aerosil (0.05 g g^{-1}) are employed to create the kidney phantoms, as shown in Fig. 5C to demonstrate that despite differences in the amount of silicone oil used in the formulations, which can adversely impact resolution (as seen before in the rheology section), incorporating fumed silica produces comparable resolution across all formulations. It is noteworthy that the printing settings used to print each formulation are the same, and the resolution remains constant. The printing of the kidney with the three formulations has been successfully accomplished while maintaining the anatomical geometry, partly owing to the kidney's inherent "self-sustainability." For manufacturing anatomical structures with highly pronounced cantilevers, it

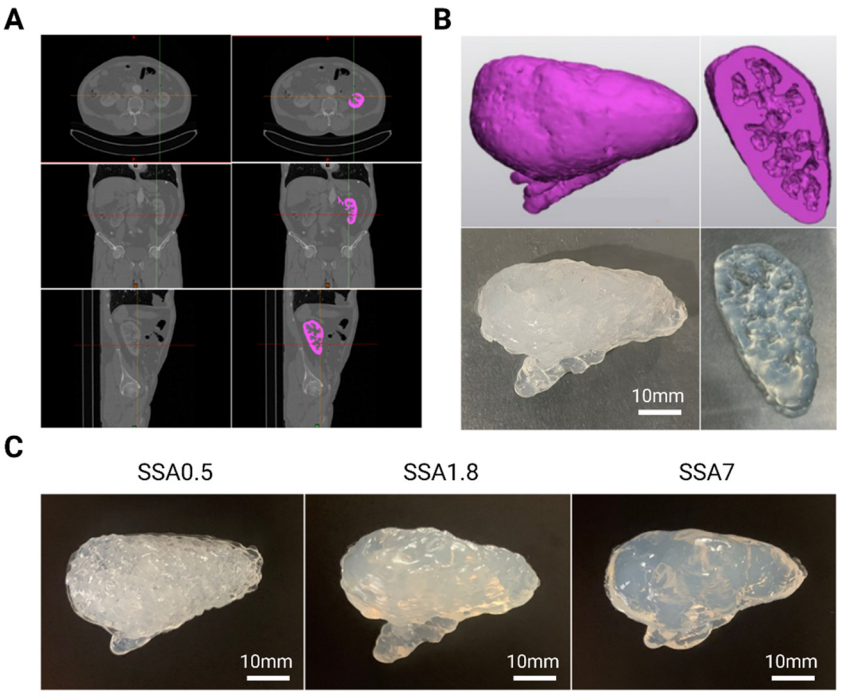

Fig. 5 Kidney phantom model. (A) Segmentation of a kidney using the specialized medical software to obtain a kidney's 3D model. (B) Comparison of the 3D kidney's model and silicone-based kidney's phantom, showing high precision of the 3D printing. (C) Comparison between the same 3D model printed with SSA0.5, SSA1.8 and SSA7 silicone formulations.

will be necessary to implement these inks in a printing technology equipped with the support material to fully exploit their potential. In this sense, this strategy can be used alone or into a different printing extrusion technology to print phantoms with different silicone formulations that can be used as a medical and surgical simulator, and as valuable tools to train practitioners, plan surgeries, and inform patients of the procedure.

3.4. Recreation of viscoelastic properties of soft tissues

After achieving fine tuning of silicone-based formulations obtaining optimum printability requirements by adding Aerosil, it is crucial that our materials have biological mechanical properties. Soft tissues have mechanical characteristics ranging from a few Pascals (Pa) to hundreds of Mega Pascals (MPa). The enormous mechanical differences between these biological soft tissues and organs must be covered by new materials. To attain the desired tissue-matching mechanical qualities, we here present a silicone-gel-based material with tissue-like softness, whose mechanical properties can be tuned over a large range by controlling the composition of the formulation and the cross-linking density of the silicone network.

Silicone mechanical properties after the curing process are evaluated to be compared with soft tissue properties. Although mechanobiology research has focused on the elastic component of soft tissue mechanical properties, soft tissues in the human body have viscoelastic behaviour.[61] Viscoelasticity is the property of materials that exhibit both viscous and elastic behaviour.[62] The elastic or storage modulus is related to the specimen's stiffness, and the viscous or loss modulus correlates with the specimen's ability to dissipate mechanical energy. For this reason, we evaluate the viscous and elastic moduli in a wide range of frequencies using dynamic mechanical analysis (DMA), to understand soft tissue mechanical properties under different conditions.

To recreate the viscoelasticity of a variety of soft tissues, the incorporation of different ratios of silicone oil has been used as a strategy to generate materials with different viscoelastic properties. As shown in Fig. 6 (left), after photopolymerization, we obtain solid viscoelastic materials in all cases considering that elastic moduli of all formulations are higher than viscous moduli. This tells us that all materials have enough consistency to be able to be handled and are correctly cured. Moreover, moduli of five orders of magnitude are achieved just by

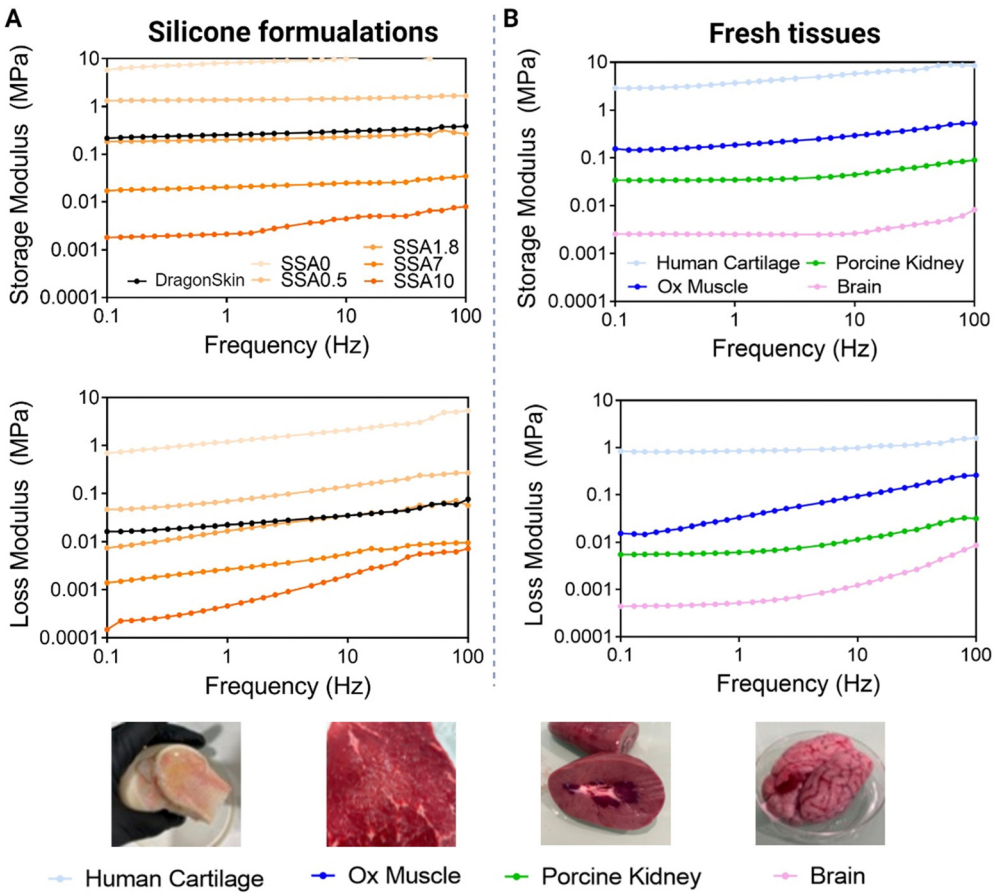

Fig. 6 Dynamic Mechanical Analysis to evaluate viscoelastic properties of silicone gel-based formulations after the curing process. (A) Compression modulus to determine silicone oil effect on viscous and elastic moduli. Formulations with ratios 0, 0.5, 1.8, 7 and 10 of silicone oil *versus* silicone are represented using an orange palette. The higher the quantity of silicone oil, the darker the orange colour. (B) Compression modulus to evaluate soft biological tissues (cartilage, muscle, kidney, and brain).

increasing the ratio between silicone oil and silicone by 10 times. Therefore, by controlling the quantity of silicone oil added, it is possible to control silicone's viscoelastic properties. This is because silicone oil is working as a plasticizer, and it acts by decreasing the interactions between the polymer chains, thereby increasing the distance between them. This results in an increase in the free volume of the material making it more flexible and less stiff.

To demonstrate if the range of viscoelastic properties obtained with our strategy is interesting to mimic soft tissues, and to ensure that the DMA method evaluates accurately viscoelasticity, different tissues are evaluated using the same method as silicone formulations. As can be observed in Fig. 6A, the storage modulus is higher that the loss modulus over the entire frequency range, validating the solid-like behaviour of the biological tissues. Lamb brain storage moduli range from 0.001 to 0.01 MPa, porcine kidney storage moduli range from 0.02 to 0.1 MPa, ox muscle range from 0.1 to 0.2 MPa, and human cartilage storage moduli range from 2 to 10 MPa. The loss moduli for lamb brain range from 0.0002 to 0.01 MPa, for a porcine kidney from 0.008 to 0.02 MPa, for ox muscle from 0.01 to 1 MPa and, for human cartilage from 1 to 10 MPa. As expected, viscoelastic moduli of cartilage are higher than those of muscle, and those of muscle are higher than those of kidney and brain. Soft tissues' value of elastic modulus ranging from 0.1 kPa to 10.000 kPa have been described in other studies[2] being the brain the organ with the lowest mechanical properties and the muscle, the tissue with one of the highest. Thus, the values obtained in our study match the recent bibliography on this topic. These results indicate first that this method can differentiate between biological tissues with diverse mechanical properties, thus, it can be used to evaluate the mechanical properties of biological tissues. Second, they give an idea of which are viscoelasticity values interesting to mimic if the focus is the reproduction of soft tissue elastic and viscous moduli.

When comparing silicone and tissue DMA, it is demonstrated that by varying the quantity of silicone oil, it is possible to mimic viscoelastic moduli of different biological tissues. SSA0 can be comparable with cartilage, SS1.8 to ox muscle, SSA7 to kidney and finally SSA10 to the brain. Thus, the strategy presented in this paper can cover a great variety of soft biological tissues' mechanical properties. Although these silicone formulations cannot fully replicate the complexity of natural tissue, the viscoelastic properties achieved using silicone oil demonstrate promising for improving the mimicking of soft tissues.

3.5. Accuracy evaluation method. Surgeons' practice

The main purpose of this study is to demonstrate the importance of the evaluation of the viscoelastic properties of materials used in the production of surgical phantoms, as they play a critical role in improving the texture and overall quality of these phantoms, when they are used as tools for planning and practising surgical

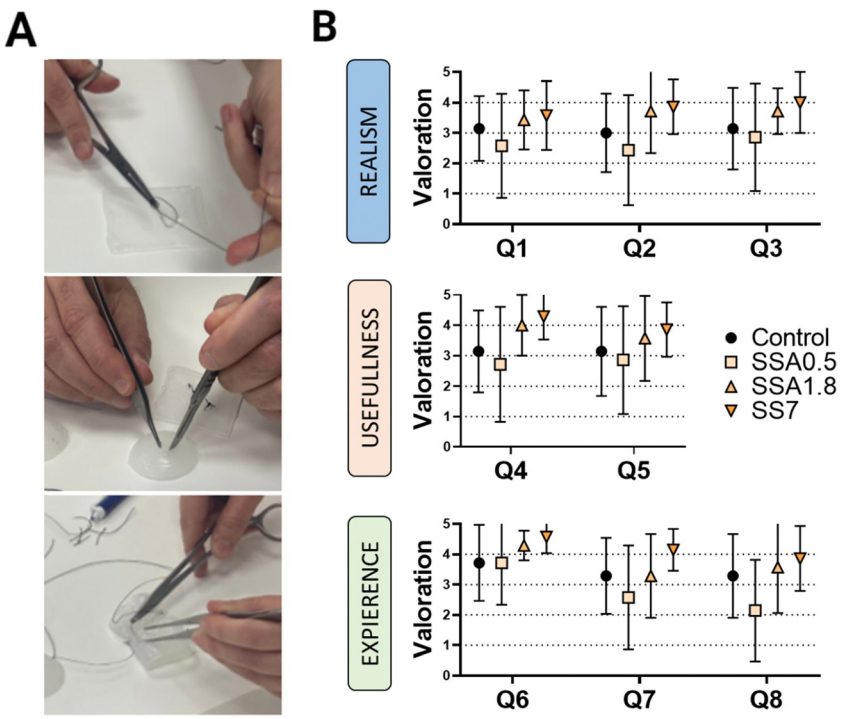

Fig. 7 Validation of materials by experienced surgeons. (A) Semi-spherical and squared samples are used to evaluate silicone-based formulations. Different cuts and sutures are performed into each sample to qualify each formulation using a protocolized questionnaire and comparing it to DragonSkin silicone. (B) Graphical representation of the results obtained from the first part of the protocolized questionnaire. Questions to evaluate fidelity (in yellow), usefulness (in green) and experience (in orange) when using these materials for rehearsing surgical plans.

Table 1 Description of the different guidelines provided to surgeons to evaluate the silicone samples to evaluate its perception in terms of realism, usefulness and experience

Evaluated perception	Guidelines provided to surgeons	Question
Realism	• The tactile sensation of the tissue is realistic.	Q1
	• The tissue behavior when cutting is realistic.	Q2
	• The behavior in suture techniques is realistic.	Q3
Usefulness	• The model is useful for educating students.	Q4
	• The material is useful for procedure planning.	Q5
Experience	• The model is easy to use.	Q6
	• The model met the needs for producing a medical phantom.	Q7
	• I would use a specific 3D anatomical model for surgical practice with this material.	Q8

procedures. To validate the DMA results and demonstrate the significance of viscoelasticity in simulating biological tissues and organs, we enlisted the feedback of seven skilled surgeons from Sant Joan de Déu Hospital. They tested our materials by suturing and cutting semi-spherical and squared samples (as shown in Fig. 7A), following a qualitative protocol that involved two phases. The first phase involved answering eight questions to assess the surgeon's perceptions when using samples of our materials printed in DIW, while the second phase involves comparing the sample being manipulated by the surgeon with their perception of manipulating different tissues and organs, studying if there is a relationship between the surgeon's sensation and the viscoelastic behaviour of the sample.

In the first phase, three categories are evaluated based on the surgeon's perception: Realism, usefulness, and experience (Table 1). The 'Realism' category aims to assess whether the surgeon considers the tactile sensation, cutting, and suturing of the different materials realistic. Thus, the surgeon's

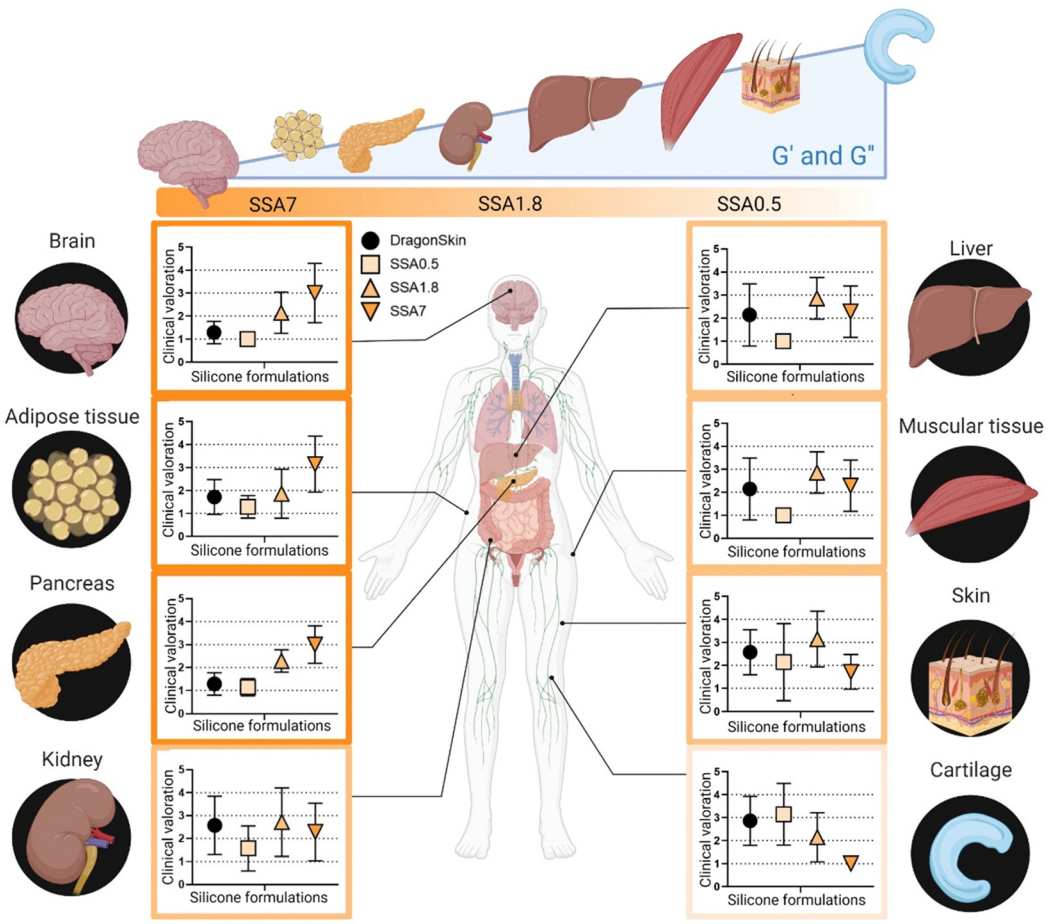

Fig. 8 Representation of similarities between different organs and tissues with DragonSkin (in black), SSA0.5 (lightest orange), SSA1.8 (middle orange) and SSA7 (darkest orange). Each of the silicone-based formulations is compared with different human organs or tissues to evaluate similarities. Surgeons' clinical validation is rated out of 5 and expressed in the Y axis and the four different silicones (SSA0.5, 1.8, 7 and DragonSkin) are represented in the X axis. The colour of the box in each graph represents the formulation with the highest score in the questionnaire.

perspective is evaluated regarding whether our strategy is perceived as 'more realistic' than the material they are accustomed to using (Dragonskin silicone). In the 'Usefulness' category, the surgeon's perception of the model's utility for educational purposes as well as surgical planning is evaluated. Finally, in the 'Experience' category, we assess the surgeon's willingness to use medical models manufactured with these materials.

Fig. 7B presents the results of each silicone formulation tested on the first part of the questionnaire. For the 'Realism' section, it is interesting to note that surgeons perceive softer materials (SSA1.8 and SS7) as more realistic, as they received higher scores in all questions of this category. This could be interpreted as surgeons considering softer materials more realistic for practicing with medical models, confirming the need to improve the functionality of current phantoms. This perception is further confirmed in the 'Usefulness' section, where surgeons also believe that softer materials would be more useful for educational purposes as well as surgical planning. Similarly, in the 'Experience' section, overall, all surgeons showed a greater predisposition to use samples SSA1.8 and SSA7 rather than the gold standard DragonSkin.

At this point, it is evident that the surgical team values the use of softer materials for recreating tissues in surgical planning. However, it remains unclear whether subtle differences in the elastic modulus of the material could be recognized from a surgeon's perception perspective when manipulating tissues. To address this, in the second phase of the questionnaire, the surgical team is required to provide their perception of similarity between the silicone-based material samples and a selection of organ tissue. The results of this second phase are shown in Fig. 8. Silicone formulation with the lowest viscoelastic moduli (SSA7) is observed to be more analogous to tissues with lower elastic and loss moduli, such as brain, adipose tissue, and pancreas. Conversely, SS1.8 appears to simulate the mechanical properties of the kidney, liver, muscular tissue, and skin, while SSA0.5 shows similarity to cartilage. This finding demonstrates that these subtle differences in the viscoelastic behaviour of the phantom's models can be detected and appreciated by the surgical team. It is interesting to observe how the respondents have a clear preference for which material more accurately recreates the behaviour to be manipulated of a soft tissue (brain, adipose tissue) or a rigid one (cartilage) but show less agreement for tissues with an intermediate modulus (liver, muscle). This reflects that, while recreating the viscoelastic behaviour of tissue represents an initial universal level of improvement in the recreation of more representative medical models, further studies should be conducted considering additional factors such as stiffness gradients inherent to each tissue peculiarities.

4. Conclusions

In summary, we have presented a refined approach to formulate silicone-based 3D inks for printing medical phantoms using DIW, employing highly accessible and widely utilized materials. Through careful control of the rheological properties *via* optimized Aerosil concentration, we have achieved precise resolution in the printed materials for producing anatomically accurate medical phantoms. Additionally, by manipulating the silicone oil concentration in the formulations, we have successfully replicated various viscoelastic patterns that mimic the distinct mechanical properties of different soft tissues. In this sense, our article presents a different perspective to the field by highlighting the use of dynamical analysis of soft tissue viscoelasticity as the pivotal characteristic to be replicated when fabricating medical phantoms for surgical practice. This perspective has been validated through surveys with a team of surgeons, obtaining evidence that a surgeon accustomed to working with medical models for surgical planning can perceive subtle changes in the viscoelastic behaviour of a model when manipulated, greatly valuing the possibility of the viscoelastic behaviour closely resembling that of the tissue to be recreated. This finding reflects the potential of our approach to markedly improve upon existing alternatives through the fabrication of 3D printed medical phantoms with a fine-tuning of its viscoelastic behaviour depending on the characteristics of the body part being recreated. Even with the limitations of survey-based methodology, it is evident that replicating viscoelastic behaviour for all tissues may not be the only factor at play, and further in-depth study is required to consider the recreation of medical models, considering the internal structural differences of each tissue. In this regard, our proposal allows for advancement in this direction, studying the implementation in higher-resolution printing systems for the micrometric recreation of these geometries, as well as the analysis of specific clinical cases to examine how our approach can facilitate the development of more realistic surgical phantoms, thereby enhancing models for medical professional training and improving the accuracy of treatment planning.

Abbreviations

3D	Three-dimensional
DIW	Direct ink writing
DMA	Dynamic mechanical analysis
SS	Silicone and silicone oil formulations
SSA	Silicone, silicone oil and Aerosil formulations
Pa	Pascals
MPa	Mega pascals
Pr	Printability rate

Conflicts of interest

There are no conflicts to declare.

Acknowledgements

The research undertaken in this paper has been partially funded by the QuirofAM project (Exp. COMRDI16-1-0011) co-financed by the

European Union through the European Regional Development Fund FEDER with the support of ACCIó-Generalitat de Catalunya 2014–2020.

References

1 C. K. McGarry, L. J. Grattan and A. M. Ivory, *et al.*, Tissue mimicking materials for imaging and therapy phantoms: A review, *Phys. Med. Biol.*, 2020, **65**(23), 23TR01, DOI: 10.1088/1361-6560/abbd17.

2 L. Schlegel, M. Ho, J. M. Fields, E. Backlund, R. Pugliese and K. M. Shine, Standardizing evaluation of patient-specific 3D printed models in surgical planning: development of a cross-disciplinary survey tool for physician and trainee feedback, *BMC Med. Educ.*, 2022, **22**(1), 1–10, DOI: 10.1186/s12909-022-03581-7.

3 M. Attaran, The rise of 3-D printing: The advantages of additive manufacturing over traditional manufacturing, *Bus Horiz.*, 2017, **60**(5), 677–688, DOI: 10.1016/j.bushor.2017.05.011.

4 A. E. Forte, S. Galvan, F. Manieri, F. Rodriguez y Baena and D. Dini, A composite hydrogel for brain tissue phantoms, *Mater Des.*, 2016, **112**, 227–238, DOI: 10.1016/j.matdes.2016.09.063.

5 M. Higgins, S. Leung and N. Radacsi, 3D printing surgical phantoms and their role in the visualization of medical procedures, *Ann 3D Print Med.*, 2022, **6**, 100057, DOI: 10.1016/j.stlm.2022.100057.

6 R. S. Libby and J. L. Silberstein, Physical Model of Clear-Cell Renal Carcinoma With Inferior Vena Cava Extension Created From a 3-Dimensional Printer to Aid in Surgical Resection: A Case Report, *Clin. Genitourin. Cancer*, 2017, **15**(5), e867–e869, DOI: 10.1016/j.clgc.2017.04.025.

7 N. Wake, J. S. Wysock, M. A. Bjurlin, H. Chandarana and W. C. Huang, ''Pin the Tumor on the Kidney:'' An Evaluation of How Surgeons Translate CT and MRI Data to 3D Models, *Urol.*, 2019, **131**, 255–261, DOI: 10.1016/j.urology.2019.06.016.

8 Ó. Girón-Vallejo, D. García-Calderón and R. Ruiz-Pruneda, *et al.*, Three-dimensional printed model of bilateral Wilms tumor: A useful tool for planning nephron sparing surgery, *Pediatr Blood Cancer*, 2018, **65**(4), 3–6, DOI: 10.1002/pbc.26894.

9 Y. L. Yap, Y. S. E. Tan and H. K. J. Tan, *et al.*, 3D printed biomodels for medical applications, *Rapid Prototyp J.*, 2017, **23**(2), 227–235, DOI: 10.1108/RPJ-08-2015-0102.

10 P. V. Glybochko, L. M. Rapoport and Y. G. Alyaev, *et al.*, Multiple application of three-dimensional soft kidney models with localized kidney cancer: A pilot study, *Urologia*, 2018, **85**(3), 99–105, DOI: 10.1177/0391560317749405.

11 Y. Zhang, H.-w Ge and N.-c Li, *et al.*, Evaluation of three-dimensional printing for laparoscopic partial nephrectomy of renal tumors: a preliminary report, *World J. Urol.*, 2016, **34**(4), 533–537, DOI: 10.1007/s00345-015-1530-7.

12 H. Lee, N. H. Nguyen, S. I. Hwang, H. J. Lee, S. K. Hong and S. S. Byun, Personalized 3D kidney model produced by rapid prototyping method and its usefulness in clinical applications, *Int. Braz. J. Urol.*, 2018, **44**(5), 952–957, DOI: 10.1590/S1677-5538.IBJU.2018.0162.

13 H. A. Atalay, V. Ülker, U. Alkan, H. L. Canat, Ü. Özkuvancl and F. Altunrende, Impact of Three-Dimensional Printed Pelvicaliceal System Models on Residents' Understanding of Pelvicaliceal System Anatomy before Percutaneous Nephrolithotripsy Surgery: A Pilot Study, *J. Endourol.*, 2016, **30**(10), 1132–1137, DOI: 10.1089/end.2016.0307.

14 C. C. Ploch, C. S. S. A. Mansi, J. Jayamohan and E. Kuhl, Using 3D Printing to Create Personalized Brain Models for Neurosurgical Training and Preoperative Planning, *World Neurosurg.*, 2016, **90**, 668–674, DOI: 10.1016/j.wneu.2016.02.081.

15 S. R. Mogali, W. Y. Yeong and H. K. J. Tan, *et al.*, Evaluation by medical students of the educational value of multi-material and multi-colored three-dimensional printed models of the upper limb for anatomical education, *Anat Sci Educ.*, 2018, **11**(1), 54–64, DOI: 10.1002/ase.1703.

16 D. S. Shin, S. H. Kang and K. H. Kim, *et al.*, Development of a deformable lung phantom with 3D-printed flexible airways, *Med. Phys.*, 2020, **47**(3), 898–908, DOI: 10.1002/mp.13982.

17 P. Morais, J. M. R. S. Tavares, S. Queirós, F. Veloso, J. D'Hooge and J. L. Vilaça, Development of a patient-specific atrial phantom model for planning and training of inter-atrial interventions, *Med. Phys.*, 2017, **44**(11), 5638–5649, DOI: 10.1002/mp.12559.

18 N. Alves, A. Kim and J. Tan, *et al.*, Cardiac Tissue-Mimicking Ballistic Gel Phantom for Ultrasound Imaging in Clinical and Research Applications, *Ultrasound Med. Biol.*, 2020, **46**(8), 2057–2069, DOI: 10.1016/j.ultrasmedbio.2020.03.011.

19 K. Wang, C. C. Ho, C. Zhang and B. Wang, A Review on the 3D Printing of Functional Structures for Medical Phantoms and Regenerated Tissue and Organ Applications, *Engineering*, 2017, **3**(5), 653–662, DOI: 10.1016/J.ENG.2017.05.013.

20 A. Leibinger, A. E. Forte and Z. Tan, *et al.*, Erratum to: Soft Tissue Phantoms for Realistic Needle Insertion: A Comparative Study (Annals of Biomedical Engineering, 10.1007/s10439-015-1523-0), *Ann. Biomed. Eng.*, 2016, **44**(12), 3750, DOI: 10.1007/s10439-016-1745-9.

21 T. Punyaratabandhu, P. C. Liacouras and S. Pairojboriboon, Using 3D models in orthopedic oncology: presenting personalized advantages in surgical planning and intraoperative outcomes, *3D Print Med.*, 2018, **4**(1), 12, DOI: 10.1186/s41205-018-0035-6.

22 P. Gareth, R. B. Emma and C. Sean, *et al.*, An open source heterogeneous 3D printed mouse phantom utilising a novel bone representative thermoplastic, *Physincs Med. Biol.*, 2020, 13Published online.

23 N. Dukov, K. Bliznakova, N. Okkalidis, T. Teneva, E. Encheva and Z. Bliznakov, Thermoplastic 3D printing technology using a single filament for producing realistic patient-derived breast models, *Phys. Med. Biol.*, 2022, **67**(4), 045008, DOI: 10.1088/1361-6560/ac4c30.

24 M. M. Mille, K. T. Griffin, R. Maass-Moreno and C. Lee, Fabrication of a pediatric torso phantom with multiple

tissues represented using a dual nozzle thermoplastic 3D printer, *J. Appl. Clin. Med. Phys.*, 2020, **21**(11), 226–236, DOI: 10.1002/acm2.13064.

25 D. P. G. Nilsson, M. Holmgren and P. Holmlund, *et al.*, Patient-specific brain arteries molded as a flexible phantom model using 3D printed water-soluble resin, *Sci. Rep.*, 2022, **12**(1), 1–9, DOI: 10.1038/s41598-022-14279-7.

26 D. Manton, M. G. Jameson and M. B. Barton, 3D printed phantoms mimicking cortical bone for the assessment of ultrashort echo time magnetic resonance imaging, *Int. J. Med. Phys. Res. Practice*, 2018, **45**(2), 758–766, DOI: 10.1002/mp.12727.

27 B. Tang, G. B. Hanna and A. Cuschieri, Analysis of errors enacted by surgical trainees during skills training courses, *Surgery*, 2005, **138**(1), 14–20, DOI: 10.1016/j.surg.2005.02.014.

28 L. Krauel, F. Fenollosa and L. Riaza, *et al.*, Use of 3D Prototypes for Complex Surgical Oncologic Cases, *World J. Surg.*, 2016, **40**(4), 889–894, DOI: 10.1007/s00268-015-3295-y.

29 B. J. Guy, A. Morris and S. A. Mirjalili, Toward Emulating Human Movement: Adopting a Data-Driven Bitmap-Based ''Voxel'' Multimaterial Workflow to Create a Flexible 3D Printed Neonatal Lower Limb, *3D Print. Addit. Manuf.*, 2022, **9**(5), 349–364, DOI: 10.1089/3dp.2021.0256.

30 W. J. Lee, Y. H. Kim and S. D. Hong, *et al.*, Development of 3-dimensional printed simulation surgical training models for endoscopic endonasal and transorbital surgery, *Front Oncol.*, 2022, **12**(August), 1–8, DOI: 10.3389/fonc.2022.966051.

31 J. Yin, M. Li, G. Dai, H. Zhou, L. Ma and Y. Zheng, 3D Printed Multi-material Medical Phantoms for Needle-tissue Interaction Modelling of Heterogeneous Structures, *J. Bionic. Eng.*, 2021, **18**(2), 346–360, DOI: 10.1007/s42235-021-0031-1.

32 M. Miyoshi, P. Punpongsanon, D. Iwai and K. Sato, SoftPrint: Investigating haptic softness perception of 3D printed soft object in FDM3D printers, *Int. Conf. Digit. Print. Technol.*, 2021, **4**(October), 78–85, DOI: 10.2352/J.ImagingSci.Technol.2021.65.4.040406.

33 S. Hatamikia, L. Jaksa, G. Kronreif and W. Birkfellner Silicone phantoms fabricated with multi-material extrusion 3D printing technology mimicking imaging properties of soft tissues in CT.

34 M. M. Nguyen, S. Zhou, J. L. Robert, V. Shamdasani and H. Xie, Development of oil-in-gelatin phantoms for viscoelasticity measurement in ultrasound shear wave elastography, *Ultrasound Med. Biol*, 2014, **40**(1), 168–176, DOI: 10.1016/j.ultrasmedbio.2013.08.020.

35 F. C. Meral, T. J. Royston and R. Magin, Fractional calculus in viscoelasticity: An experimental study, *Commun. Nonlinear Sci. Numer. Simul.*, 2010, **15**(4), 939–945, DOI: 10.1016/j.cnsns.2009.05.004.

36 N. Özkaya, D. Goldsheyder, M. Nordin and D. Leger Fundamentals of biomechanics: Equilibrium, motion, and deformation, 4th edn. *Fundam Biomech Equilibrium, Motion, Deform.*, 2016, pp. 1–454Published online, DOI: 10.1007/978-3-319-44738-4.

37 D. Liu, P. Jiang and Y. Wang, *et al.*, Engineering Tridimensional Hydrogel Tissue and Organ Phantoms with Tunable Springiness, *Adv. Funct. Mater.*, 2023, **33**(17), 2214885, DOI: 10.1002/adfm.202214885.

38 M. Wang, W. Li and J. Hao, *et al.*, Molecularly cleavable bioinks facilitate high-performance digital light processing-based bioprinting of functional volumetric soft tissues, *Nat. Commun.*, 2022, **13**(1), 1–18, DOI: 10.1038/s41467-022-31002-2.

39 T. J. Hinton, Q. Jallerat and R. N. Palchesko, *et al.*, Three-dimensional printing of complex biological structures by freeform reversible embedding of suspended hydrogels, *Sci Adv.*, 2015, **1**(9), e1500758, DOI: 10.1126/sciadv.1500758.

40 A. Leibinger, A. E. Forte and Z. Tan, *et al.*, Soft Tissue Phantoms for Realistic Needle Insertion: A Comparative Study, *Ann. Biomed. Eng.*, 2016, **44**(8), 2442–2452, DOI: 10.1007/s10439-015-1523-0.

41 S. R. Caliari and J. A. Burdick, A practical guide to hydrogels for cell culture, *Nat. Methods*, 2016, **13**(5), 405–414, DOI: 10.1038/nmeth.3839.

42 G. Rajeshkumar, R. Vishnupriyan and S. Selvadeepak, Tissue Mimicking Material an Idealized Tissue Model for Clinical Applications: A Review, *Mater Today Proc.*, 2019, **22**, 2696–2703, DOI: 10.1016/j.matpr.2020.03.400.

43 D. Hong, S. Moon, J. B. Seo and N. Kim, Development of a patient-specific chest computed tomography imaging phantom with realistic lung lesions using silicone casting and three-dimensional printing, *Sci. Rep.*, 2023, **13**(1), 1–9, DOI: 10.1038/s41598-023-31142-5.

44 M. M. Duran, G. Moro, Y. Zhang and A. Islam, 3D printing of silicone and polyurethane elastomers for medical device application: A review, *Adv. Ind. Manuf. Eng.*, 2023, **7**, 100125, DOI: 10.1016/j.aime.2023.100125.

45 R. Y. Lukin, A. M. Kuchkaev, A. V. Sukhov, G. E. Bekmukhamedov and D. G. Yakhvarov, Platinum-catalyzed hydrosilylation in polymer chemistry, *Polymers*, 2020, **12**(10), 1–22, DOI: 10.3390/POLYM12102174.

46 A. Foerster, V. Annarasa and A. Terry, *et al.*, UV-curable silicone materials with tuneable mechanical properties for 3D printing, *Mater Des.*, 2021, **205**, 109681, DOI: 10.1016/j.matdes.2021.109681.

47 T. Aziz, H. Fan, F. U. Khan, M. Haroon and L. Cheng, Modified silicone oil types, mechanical properties and applications, *Polym. Bull.*, 2019, **76**(4), 2129–2145, DOI: 10.1007/s00289-018-2471-2.

48 M. Dolz, F. Gonzlez, J. Delegido, M. J. Hernndez and J. Pellicer, A time-dependent expression for thixotropic areas. Application to Aerosil 200 hydrogels, *J. Pharm. Sci.*, 2000, **89**(6), 790–797, DOI: 10.1002/(SICI)1520-6017(200006)89:6<790::AID-JPS11>3.0.CO;2-2.

49 CIM-UPC. Direct Ink Writing. https://www.cimupc.org/en/rdi/technologies/direct-ink-writing/.

50 R. Texidó, G. Nieva-Esteve, J. Gilabert-Porres, G. Reyes and S. Borrós, Highly Sensitive Silver-Microlayer Thin Film on a pp-PFM-Modified PDMS Strain Sensor as a Versatile Tool for Stretchable Electronics Applications, *Adv. Electron. Mater.*, 2023, **9**(2), 2200717, DOI: 10.1002/aelm.202200717.

51 A. Schwab, R. Levato, M. D'Este, S. Piluso, D. Eglin and J. Malda, Printability and Shape Fidelity of Bioinks in 3D Bioprinting, *Chem. Rev.*, 2020, **120**(19), 11028–11055, DOI: **10.1021/acs.chemrev.0c00084**.

52 A. Hernández-Sosa, R. A. Ramírez-Jiménez and L. Rojo, *et al.*, Optimization of the Rheological Properties of Self-Assembled Tripeptide/Alginate/Cellulose Hydrogels for 3D Printing, *Polymers*, 2022, **14**(11), 2229, DOI: **10.3390/polym14112229**.

53 N. Paxton and W. Smolan, Proposal to Assess Printability of Bioinks for Extrusion-based Bioprinting and Evolution of Rheological Properties Governing Bioprintability, *Opt. Phys.*, 2018, 11–14.

54 M. Lanaro, J. Skewes, L. Spiers, P. K. Yarlagadda and M. A. Woodruff, Design of an open-source, low-cost bioink and food melt extrusion 3D printer, *J. Vis. Exp.*, 2020, **2020**(157), 3–15, DOI: **10.3791/59834**.

55 L. Ouyang, R. Yao, Y. Zhao and W. Sun, Effect of bioink properties on printability and cell viability for 3D bioplotting of embryonic stem cells, *Biofabrication*, 2016, **8**(3), 1–12, DOI: **10.1088/1758-5090/8/3/035020**.

56 Y. He, F. Yang, H. Zhao, Q. Gao, B. Xia and J. Fu, Research on the printability of hydrogels in 3D bioprinting, *Sci. Rep.*, 2016, **6**, 1–13, DOI: **10.1038/srep29977**.

57 S. Kyle, Z. M. Jessop, A. Al-Sabah and I. S. Whitaker, 'Printability'' of Candidate Biomaterials for Extrusion Based 3D Printing: State-of-the-Art.', *Adv. Healthc. Mater.*, 2017, **6**(16), 1–16, DOI: **10.1002/adhm.201700264**.

58 Y. Wang and N. Willenbacher, Phase-Change-Enabled, Rapid, High-Resolution Direct Ink Writing of Soft Silicone, *Adv. Mater.*, 2022, **34**(15), e2109240, DOI: **10.1002/adma.202109240**.

59 H. Chen, W.-M. Zhang, X. Li, Q. Ding and L. Shao, Direct Ink Writing of Pure PDMS for Soft 3D Microstructures and Tactile Sensors. *2021 21st International Conference on Solid-State Sensors, Actuators and Microsystems (Transducers)*, Orlando, FL, USA, 2021, pp. 525–528, DOI: **10.1109/Transducers50396.2021.9495679**.

60 H. Baniasadi, R. Abidnejad and M. Fazeli, *et al.*, Innovations in hydrogel-based manufacturing: A comprehensive review of direct ink writing technique for biomedical applications, *Adv. Colloid Interface Sci.*, 2024, **324**, 103095, DOI: **10.1016/j.cis.2024.103095**.

61 T. J. Petet, H. E. Deal, H. S. Zhao, A. Y. He, C. Tang and C. A. Lemmon, Rheological characterization of poly-dimethyl siloxane formulations with tunable viscoelastic properties, *RSC Adv.*, 2021, **11**(57), 35910–35917, DOI: **10.1039/d1ra03548g**.

62 Z. Tan, D. Dini, F. Rodriguez and A. Elia, Composite hydrogel: A high fidelity soft tissue mimic for surgery, *Mater. Des.*, 2018, **160**, 886–894, DOI: **10.1016/j.matdes.2018.10.018**.